EAI Endorsed Transactions
on Pervasive Health and Technology
Research Article EAI.EU

Unraveling the Heterogeneity of Lower-Grade Gliomas: Deep Learning-Assisted Flair Segmentation and Genomic Analysis of Brain MR Images

Irfan Sadiq Rahat[1], Hritwik Ghosh[1], Kareemulla Shaik[1], Syed Khasim[1], Gnanajeyaraman Rajaram[2]

[1]School of Computer Science and Engineering (SCOPE), VIT-AP University, Amaravati, Andhra Pradesh
[2]Department of Applied Machine Learning, Saveetha School of Engineering, SIMATS, Chennai

Abstract

The precise identification of FLAIR abnormalities in brain MR images is essential for diagnosing and managing lower-grade gliomas, segmentation continues to be a difficult task. In this research, we develop an exhaustive strategy that integrates advanced deep learning models such as DeepLabv3, U-Net, DenseNet121-Unet, ResNet50, Attention U-Net and EfficientNet to effectively segment FLAIR abnormalities in a dataset comprising 110 lower-grade glioma patients. The cancer Imaging achieve (TCIA), includes genomic cluster data and patient-specific details. Our methodology tackles the multi-class data imbalanced by employing a customized loss function, which merges Categorical Cross Entropy (CCE) WCE and WMDL functions are used to calculate loss, allowing the network to accurately segment smaller tumor regions. By performing dense network training on 3D picture patches, the suggested technique improves detection of border region artifacts and efficiently manages storage and system limited resources. We evaluate our strategy's effectiveness on the presented dataset, emphasizing its potential for assisting correct diagnosis and individualized treatment strategies for patients with lower-grade gliomas.

Keywords: Lower-grade gliomas, Brain MR images, FLAIR abnormalities, Deep learning models, Segmentation, DeepLabv3, UNet, DenseNet121Unet, ResNet50, EfficientNet, Categorical, CCE, WCE, WMDL, Border region artifacts, 3D image patches, The Cancer Imaging Archive (TCIA), Genomic cluster data

Received on 10 July 2023, accepted on 06 September 2023, published on 29 September 2023

doi: 10.4108/eetpht.9.4016

*Corresponding author. Email: me.rahat2020@gmail.com

1. Introduction

Brain tumors result from irregular growth patterns of brain cells and can be categorized into primary or metastatic carcinomas. Glial cells such as astrocytes, ependymal cells, and oligodendrocytes give rise to primary brain tumors and may be non-cancerous or benevolent. Secondary brain tumors, on the other hand, arise from other regions of the body, such as the colon or lungs, and are frequently malignant, spreading swiftly through the circulatory system. The WHO classifies Gliomas are classified into four types, with lower-grade gliomas (LGGs) corresponding to WHO grades I and II. LGGs are characterized by slower growth and less aggressive behavior compared to high-grade gliomas (HGGs). The exact causes of brain tumors remain elusive, but genetic mutations, exposure to ionizing radiation, and altered cell growth regulation are suspected contributors. Brain tumors represent around 2% of all cancer cases, but they account for a disproportionate number of cancer-related deaths. Every year, around 24,000 new cases of the fundamental malignant brain tumors are detected in the United States alone, with a five-year survival rate of around 36% for all brain tumor types. The impact of LGGs and HGGs on patients varies depending on the tumor's location, size, and growth rate. LGGs may initially cause relatively mild symptoms such as headaches, seizures, or cognitive

changes but can eventually progress to HGGs if left untreated. HGGs, on the other hand, can cause severe symptoms and neurological deficits, affecting a person's ability to think, speak, and move. Additionally, HGGs are more challenging to treat due to their aggressive nature and resistance to conventional therapies. Consequently, brain tumor diagnosis and classification are crucial for generating appropriate treatment options and optimizing patient outcomes. Diagnosing brain tumors involves evaluating a patient's clinical history, symptoms, and various imaging procedures, CT scans, angiograms, and MRI are among examples. MRI is the preferred imaging modality for detecting gliomas due to its high-resolution capabilities and ability to provide detailed information about the tumor's size, location, and heterogeneity. FLAIR (fluid-attenuated inversion recovery) is an MRI sequence often used in glioma detection for its capacity to suppress cerebrospinal fluid signals and enhance the visibility of lesions. Manual segmentation of tumor areas in MRI scans is the current clinical practice standard. This method, however, is time-consuming and can be vulnerable to inter-observer variability. DL methods' quick improvements provide a chance to develop automated and accurate methods for brain tumor segmentation, localization, and volumetric analysis. In this research, we suggest DL-assisted Techniques for segmentation of whole tumors in brain MR images with a focus on lower-grade gliomas. The suggested approach integrates cutting-edge designs, such as DeepLabV, U-Net, DenseNet121_UNet, ResNet50, Attention U-Net, and EfficientNet. Our significant contributions are as follows: The creation of a sophisticated framework for accurately locating and segmenting regions that are relevant in brain MR images, classifying each 3D pixel/voxel as background or whole tumor. Comparative analysis of various DL algorithms to identify the most suitable model for lower-grade glioma segmentation. Addressing the limitations of existing methods through advanced techniques including patch-based classification, dense data enhancement, and a mix of weighted multi-class dice loss and cross entropy loss formulation.

1.1 Epidemiology

The field of epidemiology examines the distribution, frequency, and determinants of health conditions in specific populations. When it comes to LGGs and HGGs, epidemiological research is focused on understanding the prevalence, incidence, risk factors, and potential origins of these brain tumors. Gaining insights into the epidemiology of LGGs and HGGs is essential for devising prevention tactics, early detection methods, and tailored treatments that may help alleviate the impact of these diseases. LGGs and HGGs are connected through their source and progression. Both forms of gliomas arise from glial cells in the brain, and untreated LGGs can progress to HGGs. However, LGGs and HGGs exhibit differences in their aggressiveness, growth speed, and clinical outcomes, with HGGs generally yielding a worse prognosis.

The precise causes of LGGs and HGGs remain unclear. Nevertheless, epidemiological studies have pinpointed several risk factors associated with these brain tumors. Some of these factors include:

- **Genetic factors:** Inherited genetic conditions, such as neurofibromatosis, Li-Fraumeni syndrome, and tuberous sclerosis, may increase the likelihood of glioma development.
- **Exposure to Ionizing Radiation:** High levels of ionizing radiation exposure, which may result from radiation therapy for other cancers or work-related exposure, are correlated with a heightened glioma risk.
- **Age:** Glioma incidence typically rises with age, with LGGs more frequently diagnosed in younger adults and HGGs more common among older individuals.
- **Sex:** Gliomas are slightly more prevalent in males than females, with the gap more pronounced for HGGs.
- **Immune System Factors:** Some research suggests that individuals with a history of allergies or autoimmune diseases might have a lower glioma risk, implying that the immune system could play a role in glioma development.

Despite identifying these risk factors, most glioma cases cannot be traced to specific causes. Ongoing epidemiological research aims to discover additional risk factors and potential causal links to enhance our knowledge of LGGs and HGGs, which could ultimately lead to improved prevention and treatment approaches.

1.2 Diagnosis

In order to identify LGGs and HGGs, a systematic diagnostic process is undertaken. This involves analyzing a patient's medical background, conducting a thorough physical examination, and performing various diagnostic tests. The aim of this process is to confirm a brain tumor's existence, establish its grade, and develop an appropriate treatment strategy. The following steps are typically taken for an accurate diagnosis:

- **Evaluation of Medical History and Physical Examination:** The doctor initiates the diagnostic process by reviewing the patient's medical history, discussing symptoms, and carrying out a physical examination. During this assessment, neurological

functions such as vision, hearing, balance, coordination, strength, and reflexes may be evaluated.

- **Imaging Studies:** When a brain tumor is suspected, imaging tests become crucial for determining the tumor's size, location, and features. Common imaging techniques include:

a) **MRI:** MRI scans generate detailed brain images and are instrumental in detecting gliomas. These scans may involve specific sequences like T1-weighted, T2-weighted, and fluid-attenuated inversion recovery (FLAIR) imaging techniques are used to improve tumor visualization.

b) **Computed Tomography (CT) Scan:** Although not as detailed as MRIs, CT scans may be used when MRI is not suitable or accessible. CT scans can also identify calcification, bleeding, or hydrocephalus related to brain tumors.

c) **PET Scan:** PET scans can help distinguish tumor grades, assess tumor metabolism, or evaluate the efficacy of treatments.

- **Biopsy:** A biopsy entails extracting a small tissue sample from the tumor for microscopic examination. A neuropathologist examines the sample to classify the tumor type and grade, which is essential for devising a treatment plan. Biopsies can be conducted through:

a) **Stereotactic Needle Biopsy:** A minimally invasive method that uses a needle guided by imaging and a frame or frameless system to reach the tumor.

b) **Open Biopsy:** Executed during a craniotomy, where part of the skull is removed to access the tumor. This approach is generally employed when surgical resection is also planned.

- **Molecular testing:** Molecular testing offers additional insight into the tumor's genetic and molecular properties, which can aid in determining treatment options or predicting prognosis.

After confirming a glioma diagnosis, the medical team considers several factors, such as tumor grade, location, size, and the patient's overall health, to create a personalized treatment strategy. Contemporary imaging methods, like MRS and PET imaging, hold promise for enhancing diagnostic capabilities. Nevertheless, the current gold standard for diagnosing and grading LGGs continues to be the histopathological examination of tissue samples **[Fig.1].**

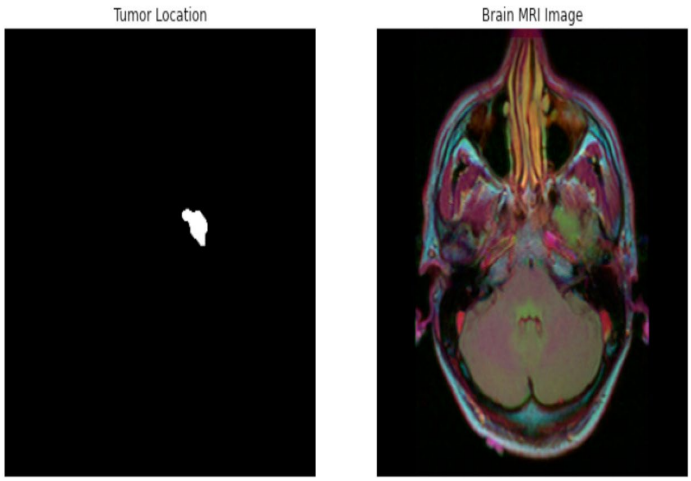

Figure 1. Tumor Location and Brain MRI Image

2. Related Works

Over the past ten years, there has been a substantial advancement in the development of image processing algorithms. A Least Squares Support Vector Machine (LS-SVM) method for segmenting images based on colour and texture was demonstrated by Yang et al. **[1].** U-Net, a well-liked Convolutional Neural Network (CNN) model, was used by Kumar et al. **[2]** and Khorasani et al. **[3]** for brain tumour identification and segmentation in magnetic resonance imaging (MRI). Both the dual feature extraction method and the integration of diffusion-weighted pictures improved the model.In the years that followed, researchers kept investigating and enhancing the U-Net model's application. A clever method for glioma segmentation in MRIs was put out by Sohail et al. **[4]** utilising a modified U-Net model.

A twofold attention U-Net was created by Li and Ren **[5],** improving the segmentation accuracy. An ACU-Net network was suggested by Tan et al. **[6]** for multimodal MRI brain tumour segmentation. The use of U-Net was further expanded by Kihira et al. **[7]** and Dong et al. **[8]** for the automatic detection of brain tumours and glioma, respectively. Ronneberger et al. introduced the U-Net architecture for biological image segmentation **[9]**. Içek et al. **[10]** then updated the architecture for dense volumetric segmentation. Artificial neural networks were used by Isensee et al. **[11]** to create an automated brain extraction approach for multisequence MRI. Kamnitsas et al. **[12]** developed an effective multi-scale 3D CNN with fully connected CRF for precise brain lesion segmentation in the wake of this study. Using deep neural networks, Havaei et al. **[13]** made additional contributions to the field of brain tumour segmentation. By adding expert segmentation labels, radiomic characteristics, and brain tumour segmentation using CNNs in MRI images, Bakas et al. **[14]** and Pereira et al. **[15]** concentrated on improving the Cancer Genome Atlas

glioma MRI collections. Menze et al.'s creation of the Multimodal Brain Tumour Image Segmentation Benchmark (BRATS) **[16]** made a contribution to the area.

Zhou et al. **[17]** introduced UNet++, a nested U-Net architecture for medical image segmentation. Deep Convolutional Neural Networks (DCNNs) were used for ImageNet classification by Krizhevsky et al. **[18].** LeCun et al. **[19]** reviewed deep residual learning for image recognition by Kaiming He et al. **[21],** which was followed byDL for large-scale picture recognition by Simonyan and Zisserman **[20].**Szegedy et al.'s **[22]** proposal for an architecture that uses convolutions to get deeper. Batch normalisation was introduced by Ioffe and Szegedy **[23]** to quicken deep network training by minimising internal covariate shift. The selection of the ideal loss function for multi-label emotion classification was the main emphasis of Hurtado Oliver et al.'s study **[24].** Hinton et al. **[25]** suggested that feature detector co-adaptation might be avoided to enhance neural networks. Kingma and Ba **[26]** introduced Adam, a stochastic optimisation technique. Dice proposed metrics of the degree of ecological interaction between species in his works **[27]** and **[30].** A better N3 Bias Correction technique, N4ITK, was created by Tustison et al. [28]. Based on a spatial overlap measure, Zou et al. **[29]** produced statistical validation of image segmentation quality. With a focus on brain tumour identification and segmentation in MRIs, this extensive collection of references offers a thorough understanding of the developments in image processing and segmentation techniques. U-Net and other deep learning models have seen substantial improvement and change throughout their growth.

3. Description of the Dataset

This study's dataset includes brain MR images as well as individually segmented FLAIR abnormality masks. These images have been obtained from TCIA and include data from 150 patients who are part of TCGA lower-grade glioma collection. Each of these patients has FLAIR sequences and available genomic cluster data. The data.csv file accompanying the dataset provides essential information on tumor genomic clusters and patient-specific data. This dataset serves as a valuable resource for the research paper, allowing for a comprehensive analysis of lower-grade glioma cases and their association with radiogenomic factors.

3.1 Image Resizing

Image resizing is an essential preprocessing step in which the original MR images and their corresponding FLAIR abnormality segmentation masks are adjusted to have the same dimensions. This process ensures that all images in the dataset have the same resolution, allowing for consistent processing and analysis throughout the study.Resizing the images involves selecting a target dimension (width and height) and applying a resizing algorithm to change the size of each image accordingly. Common algorithms for resizing images include nearest-neighbor interpolation, bilinear interpolation, and bicubic interpolation. These techniques operate by predicting the intensity measurements for pixels in the scaled image based on the values of the pixels of the original image. In terms of medical imaging, it is crucial to maintain the aspect ratio during resizing to preserve the original spatial relationships between anatomical structures. Depending on the dataset, isotropic resizing can be applied, where the same scaling factor is used for both width and height, ensuring that the aspect ratio is preserved. By resizing all images in the dataset to a consistent dimension, the research paper ensures uniformity across all images, streamlining the processing and analysis steps and allowing for a more accurate assessment of the categorization model's effectiveness.

3.2 Data Normalization

Data normalization is a crucial preprocessing step in medical imaging, addressing variations in MR image intensity values caused by differences in devices, acquisition methods, or patient factors. It scales intensity values to a standard range, such as 0 to 1 or a distribution known as a Gaussian with a mean of zero and a standard deviation of one is used thus reducing disparities between images and facilitating more efficient learning for the segmentation model. Common normalization techniques include min-max scaling, standard score scaling, and percentile-driven scaling. By normalizing the data set's intensity values, the research paper ensures the segmentation model's improved performance and enhanced accuracy of the results.

3.3 Data Augmentation

For the dataset used in this research, to boost the diversity and amount of the accessible data, data augmentation techniques were used. Since the dataset consists of brain MR images, the augmentation methods were carefully chosen to preserve the essential features and characteristics of the images while generating new samples. Some of the applied transformations included rotations, translations, scaling, flips, and intensity changes. By incorporating these augmentations, the model could learn more robust features from the dataset and become more invariant to variations in the provided data. Consequences Data augmentation reduced over fitting and enhanced model generalization, resulting in better and dependable segmentation results for the individual brain MR images.

3.4 Splitting the Dataset

In this research, the dataset of brain MR images was divided into three distinct sets to effectively train, validate, and evaluate the performance of the segmentation model. The dataset was divided into three parts: training, verification, and testing. The model for segmentation was trained using a training set that contained 70% of the data that was accessible. The validation test set, which included 15% of the data, was used to track the model's results during training, change hyperparameters, and confirm that the model was not overfitting. Finally, the remaining fifteen percent of the dataset was utilised to evaluate the efficacy of the model on previously unknown information, giving an unbiased review of the segmentation algorithm's effectiveness.

Feature Encoding

For this study, feature encoding was carried out to effectively convert the brain MR images and related segmentation masks into a numerical format that the segmentation model could process. After preprocessing, resizing, and normalizing the MR images to ensure consistent data representation, the pixel values of the images were transformed into numerical arrays. This step allowed the deep learning model to work with the data effectively. Similarly, the segmentation masks were translated into a numerical format, with individual pixel values denoting the existence or absence of a tumor in the image. By doing so, the model was able to extract meaningful patterns from the dataset, ultimately enhancing its capacity to accurately identify and segment tumors in brain MR images.

Feature Selection

In the context of this study, feature selection is an essential step to ensure that the most informative and relevant features from the brain MR images are utilized by the segmentation model. By focusing on the most important characteristics of the images, the model's performance can be improved, and the risk of overfitting can be reduced. To achieve effective feature selection, various techniques can be employed, such as statistical methods, filter methods, wrapper methods, or embedded methods. These techniques analyze the relationship between the features and the target variable (i.e., the segmentation masks) to determine which features contribute the most to the model's performance. For this dataset, an appropriate feature selection method would be applied to the pre-processed brain MR images, aiming to identify the most significant features that can aid in accurate tumor segmentation. By selecting the most relevant features, the segmentation model's efficiency and accuracy can be maximized, ultimately leading to improved results in the identification and segmentation of LGGs in brain MR images.

4. Image Masking

Image masking is an important preprocessing step in the analysis of brain MR images for tumor segmentation. It involves the process of isolating the region of interest (ROI) in the image while hiding or removing the irrelevant areas. In this study, image masking is applied to the brain MR images to focus on the tumor regions and exclude the surrounding non-tumor tissues, thereby improving the model's performance in detecting and segmenting the LGGs. By applying a mask to the brain MR images, the segmentation model can concentrate on the tumor regions, reducing the amount of noise and irrelevant information that might negatively impact its performance. In this research, an image masking technique will be employed to isolate the tumor regions in the dataset, and a visual representation of the masked images will be provided to demonstrate the effectiveness of this preprocessing step. By using image masking in conjunction with other preprocessing techniques, the model's efficiency and accuracy can be further enhanced, ultimately leading to improved results in the identification and segmentation of LGGs in brain MR images**[Fig.2].**

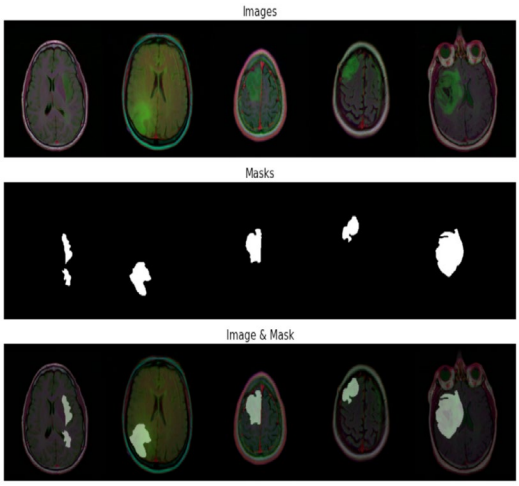

Figure 2. Image Masking

4.1 U-Net

U-Net is a specialized CNN architecture created for biomedical image segmentation problems. The U-Net architecture is made up of an encoder-decoder arrangement with connections that skip, which enable the efficient learning of high-resolution features and the precise localization of target regions, such as tumors in brain MR images. In the context of the provided dataset, U-Net's performance was not optimal, with a loss of 0.6900 and a

dice coefficient of 0.3504. This may be due to the inherent challenges in segmenting lower-grade gliomas or the need for model fine-tuning. Nevertheless, U-Net's architecture has proven successful in various medical image segmentation tasks, and further optimization or adaptation may lead to improved results for lower-grade glioma segmentation in brain MR images.

4.2 DeepLabV (versions 1, 2 and 3)

DeepLabV is a series of CNN architectures designed for tasks requiring semantic picture segmentation. The DeepLabV models employ atrous (dilated) convolutions. This allows the models to capture multi-scale contextual data as well as precisely identify regions that are intriguing in input photos such as tumor regions in brain MR images **[Fig.3]**

- **DeepLabV1:** The first version of the DeepLabV series introduced atrous convolutions to capture contextual information at different scales. In the provided dataset, DeepLabV1 achieved a loss of 0.1845 and a dice coefficient of 0.8413, demonstrating its potential in segmenting lower-grade gliomas.

- **DeepLabV2:** Building upon DeepLabV1, The second version added ASPP to capture more multi-scale context information. DeepLabV2 achieved a loss of 0.2183 and a dice coefficient of 0.8068 on the dataset, indicating its effectiveness in segmenting lower-grade gliomas.

- **DeepLabV3:** The third version of the series refined the ASPP module and incorporated image-level features to enhance the model's ability to capture global context. DeepLabV3 achieved a loss of 0.2060 and a dice coefficient of 0.8177 on the dataset, demonstrating improved performance in segmenting lower-grade gliomas compared to DeepLabV2.

- **DeepLabV3+:** DeepLabV3+ is an advanced version of the DeepLabV series, designed to improve semantic image segmentation. Building upon the atrous convolutions used in previous DeepLabV models, DeepLabV3+ Adds a decoder module to improve categorization results, especially at boundaries of objects. The decoder module enhances the model's ability to capture fine details and accurately delineate tumor regions in the provided dataset. However, the performance of DeepLabV3+ on the dataset was not as strong as some other models, with a loss of 0.3804 and a dice coefficient of 0.6517. Despite these results, DeepLabV3+ demonstrates potential in brain MR image segmentation tasks, and further optimization or combination with other models may lead to improved performance for lower-grade glioma segmentation.

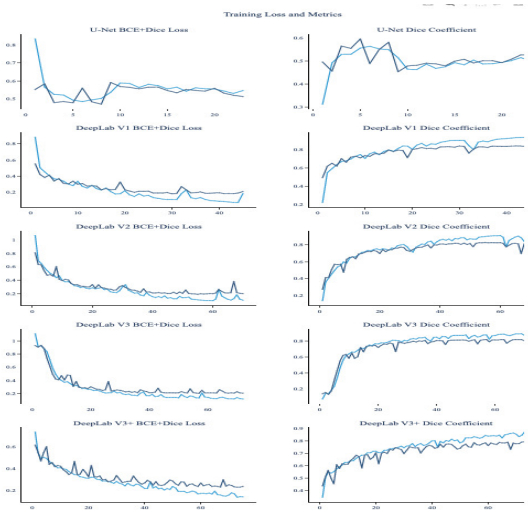

Figure 3. DeepLabV(Version 1,2 and 3)

4.3 DenseNet121_UNet

The DenseNet121_UNet model is a fusion of DenseNet121, a powerful CNN-based image categorization architecture, and the U-Net architecture specifically designed for segmentation tasks. This hybrid model leverages the strengths of both architectures, combining DenseNet121's ability to learn complex hierarchical features with U-Net's encoder-decoder structure and skip connections, which enable efficient high-resolution feature learning and precise localization of target regions in the input image. On the provided dataset of brain MR images, DenseNet121_UNet demonstrated strong performance in segmenting lower-grade gliomas. The model achieved a dice coefficient of 0.8523 and an IoU of 0.7463 on the validation dataset, indicating its effectiveness in accurately delineating tumor regions. The DenseNet121_UNet model shows promise as a robust solution for lower-grade glioma segmentation tasks, and further optimization or integration with other techniques may enhance its performance even further **[Fig.4,5].**

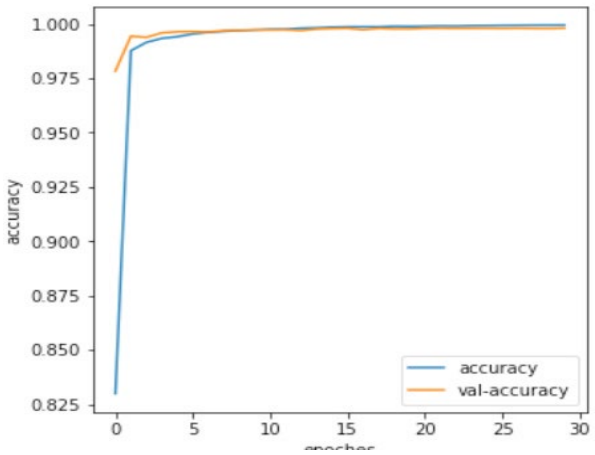

Figure 4. Accuracy of DenseNet121_UNeT

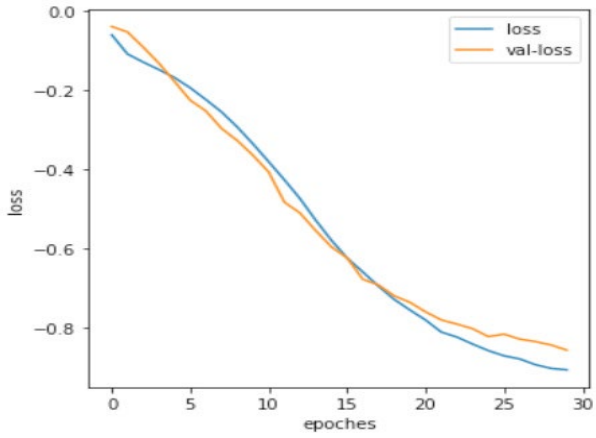

Figure 5. Loss of DenseNet121_UNeT

4.4 ResNet50

ResNet50 is a deep CNN architecture that employs excrescent learning to address the vanishing gradient problem commonly encountered in deep networks. By incorporating excrescent combinations, which approve the network to learn excrescent functions and facilitate the flow of information through the network, ResNet50 can learn complex hierarchical features and maintain high performance even with increased network depth. In the context of the provided dataset of brain MR images, ResNet50 demonstrated solid performance in segmenting lower-grade gliomas. The model achieved a loss of 0.1728 and a Tversky index of 0.9035, indicating good segmentation accuracy and the ability to accurately delineate tumor regions. ResNet50's success in this task can be attributed to its robust architecture and the benefits of residual learning. Further optimization or combination with other models may lead to improved performance in lower-grade glioma segmentation tasks **[Fig.6].**

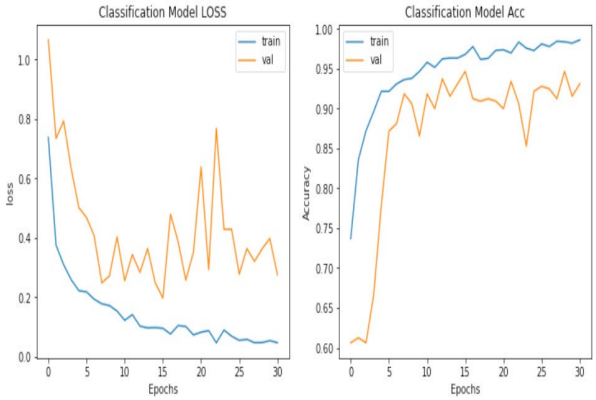

Figure 6. Loss and accuracy of ResNet50

4.5 Attention U-Net

The Attention U-Net design is an expansion of the conventional U-Net structure, incorporating attention mechanisms to enhance its segmentation capabilities. Attention mechanisms enable the model to concentrate on particular areas of interest in the picture input, such as tumor regions in brain MR images, by weighting the feature maps in the encoder-decoder structure. This allows the model to prioritize relevant features and suppress irrelevant information, leading to improved segmentation accuracy. In the context of the provided dataset of brain MR images, the Attention U-Net model demonstrated reasonable performance in segmenting lower-grade gliomas. The model achieved a loss of 0.0321, a dice coefficient of 0.2757, and an IoU of 0.1621. Although the performance metrics are not as strong as some other models, the attention mechanisms employed by Attention U-Net provide a valuable approach to enhance segmentation capabilities. Further optimization, adaptation, or integration with other techniques may lead to improved performance in lower-grade glioma segmentation tasks **[Fig.7].**

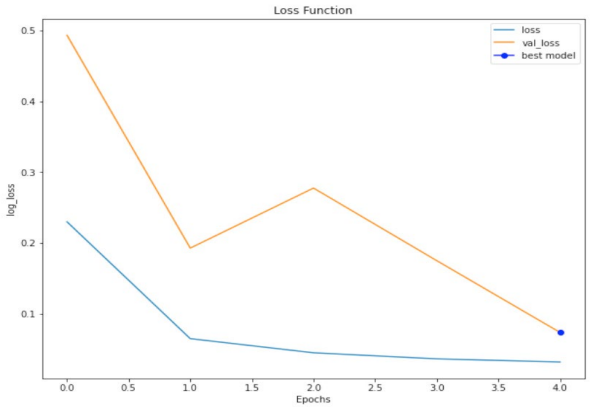

Figure 7. Loss Function of Attention U-Net

4.6 EfficientNet

EfficientNet is a family of convolutional neural networks (CNNs) that leverage a new scaling strategy for balancing network depth, size, and resolution. By optimizing the model architecture and scaling parameters, EfficientNet achieves state-of-the-art performance in various CV tasks, including image classification and segmentation. In the context of the provided dataset of brain MR images, EfficientNet demonstrated strong performance in segmenting lower-grade gliomas. The model achieved a training loss of 0.00189, a validation loss of 0.00669, an IoU of 0.8955, and a dice coefficient of 0.9237. These performance metrics indicate that EfficientNet is highly effective in accurately delineating tumor regions within the dataset.EfficientNet's success in this task can be attributed to its balanced architecture and optimized scaling, which allows the model to learn complex hierarchical features while maintaining computational efficiency. Further optimization or combination with other models may lead to even better performance in lower-grade glioma segmentation tasks **[Fig.8].**

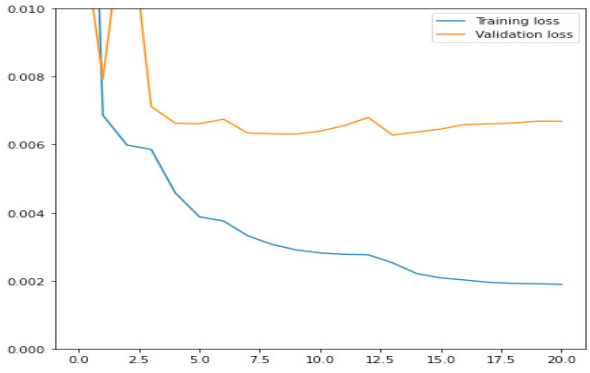

Figure 8. Training Loss and Validation Loss of EfficientNet

A detailed comparison of the varied models' efficiency on the lower-grade glioma segmentation task using the provided dataset of brain MR images reveals that some models performed better than others. EfficientNet demonstrated the best dice coefficient success of 0.9237 and an IoU of 0.8955, making it the top-performing model for the task. ResNet50 showed strong performance with a Tversky index of 0.9035, suggesting good segmentation accuracy. DenseNet121_UNet achieved a dice coefficient of 0.8523 and an IoU of 0.7463, demonstrating reasonable segmentation capabilities. DeepLabV1 ranked fourth in performance with a dice coefficient of 0.8413 and a loss of 0.1845. DeepLabV3 and DeepLabV2 achieved dice coefficients of 0.8177 and 0.8068, respectively. Attention U-Net, with a dice coefficient of 0.2757 and a loss of 0.0321, ranked seventh in performance, while U-Net had the lowest performance among the compared models with a dice coefficient of 0.3504 and a loss of 0.6900. In summary, EfficientNet and ResNet50 outperformed the other models in segmenting lower-grade gliomas in brain MR images **[Fig.9].** However, each model has its own strengths and limitations, and further optimization or integration with other techniques may lead to improved performance in lower-grade glioma segmentation tasks.

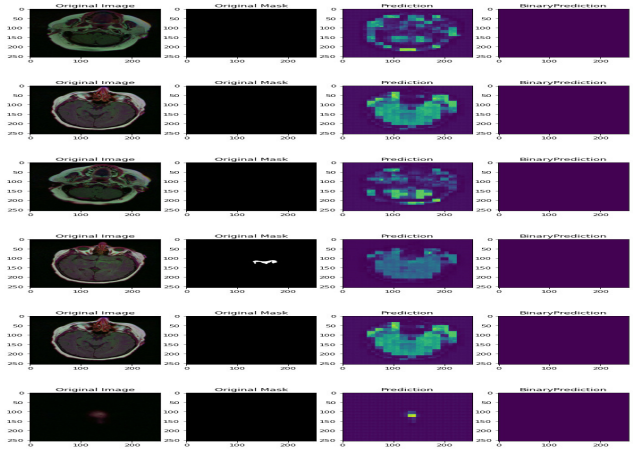

Figure 9. Presents examples of different MRI image weights and corresponding masks

5. Result

We researched the efficacy of several DL models in this study, including DeepLabv3, U-Net, DenseNet121-Unet, ResNet50, Attention U-Net, and EfficientNet, for segmenting FLAIR abnormalities in brain MR images of lower-grade gliomas. The dataset comprised 110 lower-grade glioma patients, obtained from The Cancer Imaging Archive (TCIA), with accompanying genomic cluster data

and patient-specific details. We employed a customized loss function, which combined Categorical Cross Entropy (CCE) loss, WCE, and WMDL to address the multi-class data imbalance and improve segmentation accuracy for smaller tumor regions. The results demonstrated that some models performed better than others in terms of dice coefficient, IoU, and loss values. EfficientNet emerged as the top-performing model with a dice coefficient of 0.9237 and an IoU of 0.8955, followed closely by ResNet50 with a Tversky index of 0.9035. DenseNet121-Unet, DeepLabv3, and DeepLabv1 also showed reasonable segmentation capabilities. However, U-Net and Attention U-Net exhibited lower performance metrics compared to the other models. Our proposed strategy successfully detected border region artifacts and efficiently managed memory and system resource limitations by implementing dense network training on 3D image patches. The performance comparison of different segmentation methods revealed the potential of our approach in supporting accurate diagnosis and individualized treatment strategies for patients with lower-grade gliomas. Further optimization or integration of these models with other techniques may lead to even better performance in lower-grade glioma segmentation tasks in the future.

6. Conclusion

Finally, this work looked into the effectiveness of various DL models for segmenting lower-grade gliomas in brain MR images. This study used brain MR images with customized FLAIR abnormality segmentation masks gained from TCIA and corresponding to 150 patients with lower-grade gliomas. The models compared included EfficientNet, ResNet50, DenseNet121_UNet, DeepLabV1, DeepLabV2, DeepLabV3, Attention U-Net, and U-Net. Our findings revealed that EfficientNet and ResNet50 were the top-performing models in this task, demonstrating the efficient of DL techniques to improve the segmentation of lower-grade gliomas in brain MR images. Although some models, for example Attention U-Net and U-Net, demonstrated lower performance, they still have the potential for improvement through further optimization or integration with other techniques. The findings of this study help to the ongoing research in the field of medical image analysis, particularly in the context of brain tumor segmentation. The insights gained from the performance comparison of these models can help guide future research towards developing enough accurate and efficient techniques for lower-grade glioma segmentation. This, in turn, can contribute to better treatment planning, improved patient outcomes, and more effective clinical decision-making in the management of lower-grade gliomas.

7. References

1. Yang, H.-Y., Wang, X.-Y., Wang, Q.-Y., & Zhang, X.-J. (2012). LS-SVM based image segmentation using color and texture information. Journal of Visual Communication and Image Representation, 23(7), 1095–1112. https://doi.org/10.1016/j.jvcir.2012.07.007

2. Suresh Kumar, R., Nagaraj, B., Manimegalai, P., & Ajay, P. (2022). Dual feature extraction based convolutional neural network classifier for magnetic resonance imaging tumor detection using U-Net and three-dimensional convolutional neural network. Computers & Electrical Engineering, 101, 108010. https://doi.org/10.1016/j.compeleceng.2022.108010

3. Khorasani, A., Kafieh, R., Saboori, M., & Tavakoli, M. B. (2022). Glioma segmentation with DWI weighted images, conventional anatomical images, and post-contrast enhancement magnetic resonance imaging images by U-Net. Physical and Engineering Sciences in Medicine, 45(3), 925–934. https://doi.org/10.1007/s13246-022-01164-w

4. Sohail, N., Anwar, S. M., Majeed, F., Sanin, C., & Szczerbicki, E. (2021). Smart Approach for Glioma Segmentation in Magnetic Resonance Imaging using Modified Convolutional Network Architecture (U-NET). Cybernetics and Systems, 52(5), 445–460. https://doi.org/10.1080/01969722.2020.1871231

5. Li, N., & Ren, K. (2021). Double attention U-Net for brain tumor MR image segmentation. International Journal of Intelligent Computing and Cybernetics, 14(3), 467–479. https://doi.org/10.1108/IJICC-01-2021-0018

6. Tan, L., Ma, W., Xia, J., & Sarker, S. (2021). Multimodal Magnetic Resonance Image Brain Tumor Segmentation Based on ACU-Net Network. IEEE Access, 9, 14608–14618. https://doi.org/10.1109/ACCESS.2021.3052514

7. Kihira, S., Mei, X., Mahmoudi, K., Liu, Z., Dogra, S., Belani, P., Tsankova, N., Hormigo, A., Fayad, Z. A., Doshi, A., & Nael, K. (2022). U-Net Based Segmentation and Characterization of Gliomas. Cancers, 14(18), 4457. https://doi.org/10.3390/cancers14184457

8. Dong, H., Yang, G., Liu, F., Mo, Y., & Guo, Y. (2017). Automatic Brain Tumor Detection and Segmentation Using U-Net Based Fully Convolutional Networks. In Medical Image Understanding and Analysis (Vol. 723, pp. 506–517). Springer International Publishing AG. https://doi.org/10.1007/978-3-319-60964-5_44

9. Ronneberger, O., Fischer, P., & Brox, T. (2015). U-Net: Convolutional Networks for Biomedical Image Segmentation. arXiv.org.

10. Çiçek, Özgün, Abdulkadir, A., Lienkamp, S. S., Brox, T., & Ronneberger, O. (2016). 3D U-Net: Learning Dense Volumetric Segmentation from Sparse Annotation. In Medical Image Computing and Computer-Assisted Intervention – MICCAI 2016 (pp. 424–432). Springer International Publishing. https://doi.org/10.1007/978-3-319-46723-8_49

11. Isensee, F., Schell, M., Pflueger, I., Brugnara, G., Bonekamp, D., Neuberger, U., Wick, A., Schlemmer, H., Heiland, S., Wick, W., Bendszus, M., Maier-Hein, K. H., & Kickingereder, P. (2019). Automated brain extraction of multisequence MRI using artificial neural networks. Human Brain Mapping, 40(17), 4952–4964. https://doi.org/10.1002/hbm.24750

12. Kamnitsas, K., Ledig, C., Newcombe, V. F. J., Simpson, J. P., Kane, A. D., Menon, D. K., Rueckert, D., & Glocker, B. (2017). Efficient multi-scale 3D CNN with fully connected CRF for accurate brain lesion segmentation. Medical Image Analysis, 36, 61–78. https://doi.org/10.1016/j.media.2016.10.004

13. Havaei, M., Davy, A., Warde-Farley, D., Biard, A., Courville, A., Bengio, Y., Pal, C., Jodoin, P.-M., & Larochelle, H. (2017). Brain tumor segmentation with Deep Neural Networks. Medical Image Analysis, 35, 18–31. https://doi.org/10.1016/j.media.2016.05.004

14. Bakas, S., Akbari, H., Sotiras, A., Bilello, M., Rozycki, M., Kirby, J. S., Freymann, J. B., Farahani, K., & Davatzikos, C. (2017). Advancing The Cancer Genome Atlas glioma MRI collections with expert segmentation labels and radiomic features. Scientific Data, 4(1), 170117–170117. https://doi.org/10.1038/sdata.2017.117

15. Pereira, S., Pinto, A., Alves, V., & Silva, C. A. (2016). Brain Tumor Segmentation Using Convolutional Neural Networks in MRI Images. IEEE Transactions on Medical Imaging, 35(5), 1240–1251. https://doi.org/10.1109/TMI.2016.2538465

16. Menze, B. H., Jakab, A., Bauer, S., Kalpathy-Cramer, J., Farahani, K., Kirby, J., Burren, Y., Porz, N., Slotboom, J., Wiest, R., Lanczi, L., Gerstner, E., Weber, M.-A., Arbel, T., Avants, B. B., Ayache, N., Buendia, P., Collins, D. L., Cordier, N., … Delingette, H. (2015). The Multimodal Brain Tumor Image Segmentation Benchmark (BRATS). IEEE Transactions on Medical Imaging, 34(10), 1993–2024. https://doi.org/10.1109/TMI.2014.2377694

17. Zhou, Z., Md Mahfuzur Rahman Siddiquee, Tajbakhsh, N., & Liang, J. (2018). UNet++: A Nested U-Net Architecture for Medical Image Segmentation. arXiv.org.

18. Krizhevsky, A., Sutskever, I., & Hinton, G. (2017). ImageNet classification with deep convolutional neural networks. Communications of the ACM, 60(6), 84–90. https://doi.org/10.1145/3065386

19. LeCun, Y., Bengio, Y., & Hinton, G. (2015). Deep learning. Nature (London), 521(7553), 436–444. https://doi.org/10.1038/nature14539

20. Simonyan, K., & Zisserman, A. (2015). Very Deep Convolutional Networks for Large-Scale Image Recognition. arXiv.org.

21. Kaiming He, Xiangyu Zhang, Shaoqing Ren, & Jian Sun. (2016). Deep Residual Learning for Image Recognition. 2016 IEEE Conference on Computer Vision and Pattern Recognition (CVPR), 770–778. https://doi.org/10.1109/CVPR.2016.90

22. Szegedy, C., Liu, W., Jia, Y., Sermanet, P., Reed, S., Anguelov, D., Dumitru Erhan, Vanhoucke, V., & Rabinovich, A. (2014). Going Deeper with Convolutions. arXiv.org.

23. Ioffe, S., & Szegedy, C. (2015). Batch Normalization: Accelerating Deep Network Training by Reducing Internal Covariate Shift. https://doi.org/10.48550/arxiv.1502.03167

24. Hurtado Oliver, L. F., González-Barba, J. Ángel, & Pla Santamaría, F. (2019). Choosing the right loss function for multi-label Emotion Classification.

25. Hinton, G. E., Srivastava, N., Krizhevsky, A., Sutskever, I., & Salakhutdinov, R. R. (2012). Improving neural networks by preventing co-adaptation of feature detectors. https://doi.org/10.48550/arxiv.1207.0580

26. Kingma, D. P., & Ba, J. (2014). Adam: A Method for Stochastic Optimization. https://doi.org/10.48550/arxiv.1412.6980

27. Dice, L. R. (1945). Measures of the Amount of Ecologic Association Between Species. Ecology (Durham), 26(3), 297–302. https://doi.org/10.2307/1932409

28. Tustison, N. J., Avants, B. B., Cook, P. A., Yuanjie Zheng, Egan, A., Yushkevich, P. A., & Gee, J. C. (2010). N4ITK: Improved N3 Bias Correction. IEEE Transactions on Medical Imaging, 29(6), 1310–1320. https://doi.org/10.1109/TMI.2010.2046908

29. Zou, K. H., Warfield, S. K., Bharatha, A., Tempany, C. M. C., Kaus, M. R., Haker, S. J., Wells, W. M., Jolesz, F. A., & Kikinis, R. (2004). Statistical validation of image segmentation quality based on a spatial overlap index scientific report. Academic Radiology, 11(2), 178–189. https://doi.org/10.1016/S1076-6332(03)00671-8

30. Dice, L. R. (1945). Measures of the Amount of Ecologic Association Between Species. Ecology (Durham), 26(3), 297–302. https://doi.org/10.2307/1932409

31. Ensemble Learning Framework with GLCM Texture Extraction for Early Detection of Lung Cancer on CT Images, Sara A Althubiti, Sanchita Paul, Rajnikanta Mohanty, Sachi Nandan Mohanty, Fayadh Alenezi, Kemal Polat, Computational and Mathematical Methods in Medicine (Hindawi), 2022, doi.org/10.1155/2022/2733965

32. A Novel Approach for Diabetic Retinopathy Screening Using Asymmetric Deep Learning Feature, Pradeep Kumar Jena, Bonomali Khuntia, Charulata Palai, Manjushree Nayak, Tapas Kumar Mishra, Sachi Nandan Mohanty, Big Data Cognitive Computing (2023), Vol 7, Issue 1, 25, https://doi.org/10.3390/bdcc7010025, ISSN: 2504-2289